

Tacticity in shocked polymer hydrocarbons

N. K. Bourne · J. C. F. Millett

Received: 1 June 2007 / Accepted: 26 July 2007 / Published online: 29 September 2007
© Springer Science+Business Media, LLC 2007

Abstract There is a recent interest in the response of thermoplastics to shock. Previous work on three simple hydrocarbons has indicated that the shear strength increases with the complexity of the side group. Strength values have been calculated using lateral stress measurements with manganin gauges that have been recalibrated for use in the low stress regime. The present work aims to investigate the effect of the configuration of the thermoplastic's chain when side groups are added. In particular, whether steric effects are present when the groups become larger. Results show that whilst polyethylene has the lowest shear strength, polypropylene and polystyrene have similar values. In all cases the strength of polymer increases with time after the shock has passed. As the applied stress increases, polystyrene and polypropylene strengthen to a higher degree when compared with polyethylene. Explanations are offered in terms of microstructure and tacticity of the chain.

Introduction

The response of polymers to shock propagation has received recent interest since it has become important to understand their use as binders in fibre composites, or in plastic bonded explosives (PBXs). Indeed, polystyrene is a component of the rubber binder bonding HMX grains, in the US explosives PBX-9502 and PBX-9007. Polymer microstructure, and the mechanisms by which it responds at a high strain rate and under high amplitude loading to

accommodate the compression, are surprisingly little understood. This is partly because the tools for probing microstructure are less developed in these low symmetry materials (in comparison with metals and crystals), and partly due to the paucity of investigations conducted over a range of microstructures to gain knowledge of how material constituents affect continuum response.

In this work, three polymer hydrocarbons are loaded in the low amplitude region so that a shock with induced particle velocity less than 1 km s^{-1} results. The three thermoplastics chosen are high-density polyethylene (PE), polypropylene (PP) and polystyrene (PS). The chemical form of a repeating unit in these polymers is given in Fig. 1. The simple hydrocarbon chain of polyethylene is modified in the case of polypropylene by the addition of a methyl group onto every other carbon and by the addition of a benzene ring in the case of polystyrene. The structure of the latter two chains is such that the conformation of the chain results in different bulk properties for polypropylene and polystyrene.

These thermoplastics consist of varying proportions of amorphous phase interspersed with a crystalline component composed of spherulites made up of aligned lamellae. Both PE and PP have such a form, with the PE being *ca.* 40% crystalline with slight density differences between amorphous and crystalline phases [1, 2]. Ordinary atactic polystyrene has large phenyl groups randomly distributed on both sides of the chain. Such random orientation prevents chains from aligning with sufficient regularity to achieve crystallinity. This results in the plastic having no defined melting temperature, T_m , but rather a reducing viscosity with temperature. In contrast, ordered syndiotactic polystyrene has phenyl groups on alternating sides, and is highly crystalline with a T_m of $270 \text{ }^\circ\text{C}$ [2]. Isotactic and syndiotactic polystyrene are made using catalysts that

N. K. Bourne (✉) · J. C. F. Millett
AWE, Aldermaston, Reading RG7 4PR Berkshire, UK
e-mail: Neil.Bourne@awe.co.uk

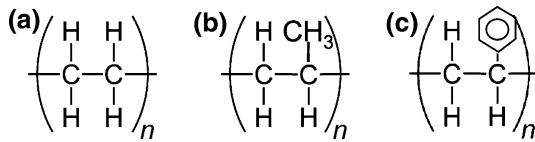


Fig. 1 Repeats unit in (a) polyethylene, (b) polypropylene (c) polystyrene chains

result in highly ordered molecular structures, however, the starting material for this work is atactic. For PS, the density of both the amorphous and the crystalline regions is 1.05 g cm^{-3} [3].

The present work aims to complete a systematic study of the continuum behaviour of the three hydrocarbons and relate the changes observed to the microstructural features discussed above. Previous work has presented data characterizing their equation of state [4]. Further experiments adding to this and mapping the deviatoric behaviour in the low-pressure region are presented here, along with an interpretation of the material response gleaned from these studies.

Materials

The polymer targets used were manufactured from commercial thermoplastics. Given the size of these experimental campaigns, they represent several batches from the same supplier. These materials will be termed stock off the shelf (SOTS) to differentiate properties from other, carefully pedigreed materials. Their properties are tabulated in Table 1 below. The PE and PP materials are believed to be *ca.* 40% crystalline and to have spherulites of size *ca.* $1 \mu\text{m}$.

Note the values of the shock constants c_0 and S are derived in the work described below.

Experimental

Plate impact experiments were performed using a 5 m long, 50 mm bore single stage gas gun [5]. There were two series of experiments. In the first, the shock stress, shock velocity and particle velocity relations were determined to deduce the equation of state. Target assemblies were made by fixing a manganin stress gauge (MicroMeasurements

type LMSS-025CH-048) between 5 or 6 mm plates of the polymers with a low viscosity epoxy adhesive. A second gauge (the 0 mm position) was supported on the front with a 1 mm plate of either aluminium alloy 6082-T6 or copper, which was matched to the material of the flyer plate. In this way, both shock stress (from the amplitude of the signal) and shock velocity through the known spacings of the gauges, in terms of position within the target assembly (Δw), and time (Δt_{shock}) could be determined ($U_s = \Delta w / \Delta t_{\text{shock}}$). Gauge calibrations were set according to Rosenberg et al. [6]. The shocks were introduced by impacting 5 mm aluminium alloy or copper flyer plates onto targets at velocities up to *ca.* 1000 m s^{-1} . The velocities of the impacting plates were deduced by measuring the shorting times of sequentially mounted pairs of pins to an accuracy of 0.5%. The particle velocity in the material behind the shock front, (u_p) was determined from the known response of the flyer plate materials [7], the measured impact velocity and longitudinal stresses from the gauges using impedance matching techniques. A second set of experiments measured the lateral component of stress (σ_y), and from that, the shear strength behind the shock front (2τ) through the relation,

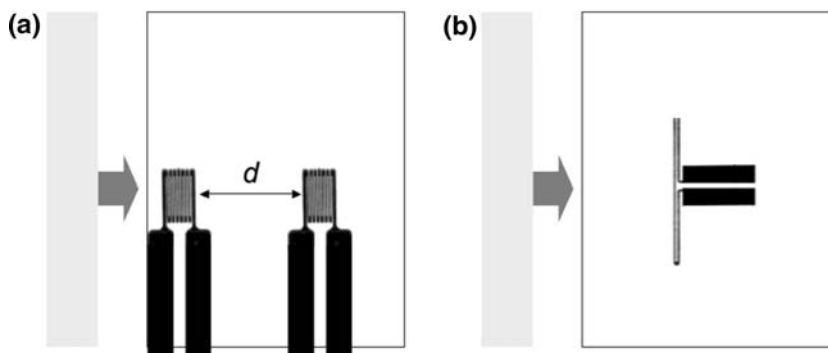
$$2 \cdot \tau = \sigma_x - \sigma_y \quad (1)$$

In this case, manganin gauges of a different type (MicroMeasurements J2M-SS-580SF-025) were introduced into sectioned 10 mm plates of the polymers, 4 mm from the impact face. The targets were re-assembled using a low viscosity adhesive, and held in a special jig for a minimum of 12 h. Afterwards, the impact face was lapped flat to no greater than 5 optical fringes from a monochromatic light source, across 50 mm. Lateral stresses were determined from the work of Rosenberg and Partom [6], using a modified analysis that does not require knowledge of the longitudinal stress [8]. Finally, the particular gauge used has a different response to the more familiar grid gauges at low stresses which was accounted for in the conversion from voltage to stress [9]. Specimen alignment was controlled by an accurately machined end-piece to the gun barrel. A schematic of specimen configurations and gauge placements are presented in Fig. 2. The acoustic properties of each polymer were measured using quartz transducers in longitudinal and shear orientation at 5 MHz, using a Panametrics PR5077 pulse receiver.

Table 1 Physical properties of the selected polymers

	$\rho \text{ kg m}^{-3}$	$c_0 \text{ m s}^{-1}$	S	$c_L \text{ m s}^{-1}$	$c_s \text{ m s}^{-1}$	Melt $T_m \text{ }^\circ\text{C}$	$T_g \text{ }^\circ\text{C}$
PE	950	2510	1.97	2460	1010	110	-100
PP	900	2770	1.54	2620	1260	175	-10
PS	1030	2290	1.64	2240	1150	-	100

Fig. 2 Schematic experimental configuration used. In (a) two longitudinal gauges placed at known separation d . In (b) lateral gauge placed 4 mm from the impact face



Results and discussion

Figure 3 shows the shock wave velocity as a function of the resulting particle velocity in the flow. The materials all show linear fits to these curves at higher particle speeds but it has been shown that these thermoplastics show some curvature at lower shock speeds for velocities less than $ca. 200 \text{ m s}^{-1}$ [10]. This is seen in Table 1 which indicates that the elastic wave speed c_L is less than the zero particle velocity value of the bulk sound speed c_0 for all three of the materials considered here. This is believed to be due to the composite nature of the microstructure where the sound speed in one of the phases drops into the elastic range whilst the amorphous surrounding phase remains hydrodynamic.

It will be seen that the slope of the fit for PE is greater than that for PP and PS. The value of S has been correlated with the first pressure derivative of the bulk modulus. This indicates the polyethylene matrix to be more compressible than PP and PS which is reasonable given their greater number of side groups.

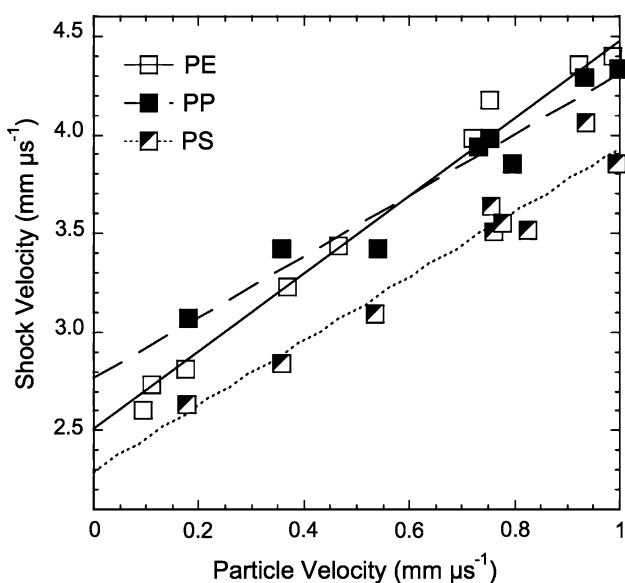


Fig. 3 Reduced U_s-u_p plot for PE, PP and PS

Table 2 shows the variation of the constants c_0 and S measured in this work and in two others [3, 4]. It will be seen that Millett fits to a data range greater than that chosen here ($<1000 \text{ m s}^{-1}$) and that Marsh derives data only for particle velocities greater than this value [7]. The totality of the data shows similar trends but emphasizes that the response is not constant over this region with both the constants varying. Only in the case of PS, are the longitudinal and bulk wave speeds approximately equal. In the other materials, c_0 is greater than c_L .

Figure 4 shows the Hugoniot curves for the three materials. In the particle velocity range chosen there is data from Carter and Marsh [3], Millett and Bourne [4]. Note that the latter data gives longitudinal stress values measured using suitable sensors. In the case of the first works, free surface velocities are measured and converted back to hydrodynamic pressure, P . These pressure points thus lie below those for stress. The shock constants, derived in Table 2 for the three polymers, are used to construct a hydrodynamic curve for each using equation 2 below.

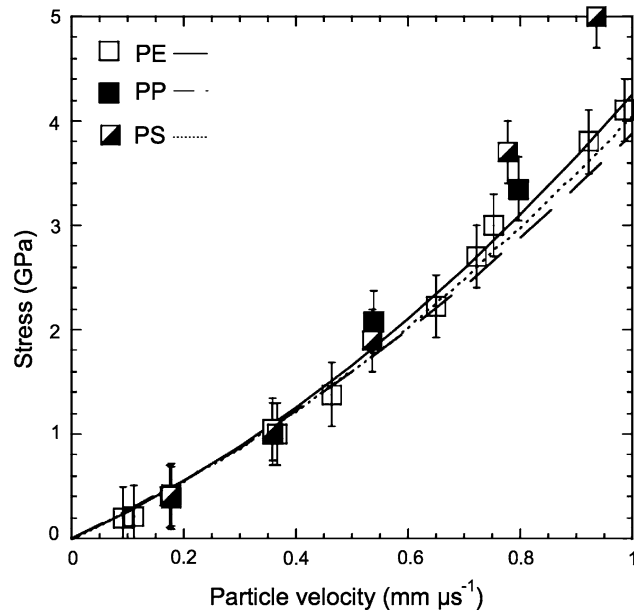
$$P = \rho_0(c_0 + Su_p)u_p \tag{2}$$

The three curves are close to one another. PE lies at the highest value of stress, then PP with PS at the base. This is due to increased values of c_0 and S for PE and its lower density. The data points lie away from these curves except for the upper two points for PE which are pressure values from Carter and Marsh [3]. The PP and the PS point lie furthest from the curves and deviate away from them at higher particle velocities. The stress values deviating away from the hydrodynamic curves for each material indicates hardening behaviour.

The lateral stress histories are presented in Fig. 5. Six typical histories at differing velocities are taken from the full set of data recorded. The histories correspond to impacts in PE, PP and PS with the following parameters. The profiles for PE were generated when copper flyer plates impacted targets at 676 and 943 m s^{-1} . Those in PP to impacts of copper flyers at 568 and 450 m s^{-1} and in PS,

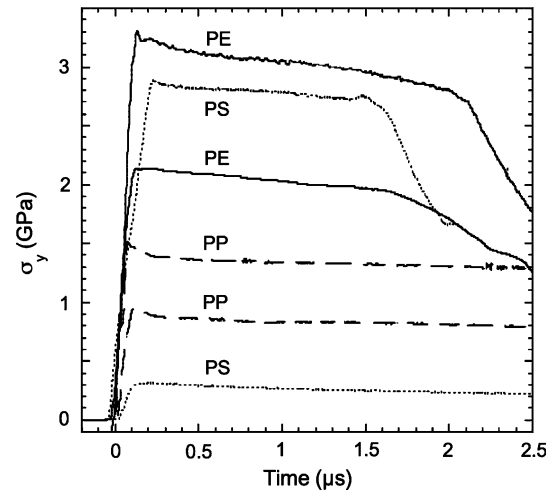
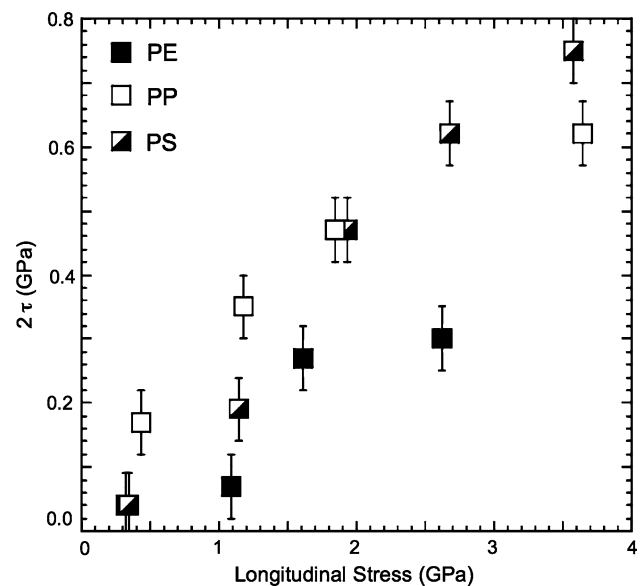
Table 2 Values of shock constants c_0 and S for the three materials

	ρ kg m ⁻³ ± 20	c_0^a m s ⁻¹ ± 20	S^a ± 0.02	c_0^b m s ⁻¹ ± 20	S^b ± 0.02	c_0^c m s ⁻¹ ± 20	S^c ± 0.02	c_L m s ⁻¹ ± 20
PE	950	2340	2.57	2860	1.57	2510	1.97	2460
PP	900	2900	1.16	2860	1.49	2770	1.54	2620
PS	1030	2210	1.84	2340	1.58	2290	1.64	2240

^a Millett and Bourne [4]^b Carter and Marsh [3]^c This work**Fig. 4** Reduced data plotted as principal Hugoniot for PE, PP and PS. Filled symbols for PP, open for PE, and half-filled markers for PS. Stress ordinate to left, shock velocity to right

copper flyer at 862 m s⁻¹ and of an aluminium alloy 6082-T6 flyer at 200 m s⁻¹. The two PE traces correspond to longitudinal stress levels (constant over the period of the pulse) of 2.5 and 1.6 GPa, those in PP to stresses of 1.3 and 0.9 GPa, and those in PS to 2.7 and 0.5 GPa determined from the Hugoniot data deduced from equation 3. In all cases the lateral stress decreases over time at an approximately constant rate regardless of the material. This rate is *ca.* 0.8 GPa μs⁻¹ at the highest shock amplitude for PE.

The histories of Fig. 5 are reduced, along with the calculated longitudinal stresses measured from the Hugoniot, to calculate the shear strength of the material using Eq. 1. Figure 6 shows the variation of twice the shear strength, calculated from the measured *initial* value of the lateral stress, versus the applied longitudinal stress. All three materials show hardening behaviour and the hardening rates are ranked in such a manner as to increase with the size of the chain side group with PS lying above PP which lies above PE. The PP and PS harden at approximately the same

**Fig. 5** Lateral stress histories for the three polymers. Solid curves for PE, large dash for PP, points for PS**Fig. 6** Plot of 2τ vs. the longitudinal stress for the three polymers

rate initially, but the PP does so less at higher stresses. As has been found elsewhere, all three of these materials collapse to zero strength at higher stress values [11].

The three materials considered in this work are simple hydrocarbon thermoplastics with similar microstructure consisting of an amorphous phase with a degree of crystallinity. This results in different elastic and plastic moduli and differing yield stress for each phase of each material. The elastic impedances of the three materials, $\rho_0 c_L$, are {PE, PP, PS} of {2340, 2360, 2310 kg m⁻² s⁻¹} and shock impedances ($\rho_0 c_0$) are {1870, 1390, 1690 kg m⁻² s⁻¹}. This reflects differing elastic and plastic behaviour. In the elastic regime, densities and moduli are similar. Further, c_L is less than c_0 for all three materials which relates to a mixed response behaviour in the low stress regime where the wave travels elastically in the crystalline region but plastically in the weaker amorphous binder. In the hydrodynamic regime, which both deform plastically, the shock impedance of PE is greatest reflecting the higher curvature of the Hugoniot for that material. This results from greater compressibility between PE chains.

The forces between the chains are of Van de Waals nature since there are no polar atoms substituted into these hydrocarbons. The PS chain will experience the largest forces of this type since there are delocalized electronic states on the attached benzene rings. As has been mentioned above, there is a higher value of S for PE. This has been related to dK/dP which reflects hydrodynamic effects, and Van de Waals forces are least for PE [10]. Iso- and syn-diotactic chains in PP and PS would increase these forces further.

The strength data shows the effects of attractive forces but also tangling in the complex chain structures that exist in the bulk. These forces are maximized when the chain has bulky side groups with the largest phenyl groups found in polystyrene in this work followed by the methyl groups on polypropylene. This correlates with higher strength recorded for PS than PP, with both greater than PE. Each individual shock front shows hardening over the microseconds of the pulse length. This time is commensurate with wave propagation times across crystallites but is found to be similar for all three thermoplastics studied.

Approximate calculations for the shock temperature rise give values of one to two hundred degrees for these impact velocities and given the three materials' specific heats. This is, of order, the melting temperature of these polymers in the ambient pressure state, which of course is not the case during these experiments. In other materials, high shock pressures have resulted in recovered microstructures with an increase in crystallinity and a change in spherulite size [12, 13][T2]. It is possible here that ordering of atactic

chains and introduction of crystallinity has occurred in PP and PS with the application of temperature and pressure.

Conclusions

A series of observations on the response of thermoplastics to simple shock has been made, tracking the results of substituting methyl and phenyl groups onto a carbon backbone. The addition results in increased strength as the side group becomes larger, which is believed to be a reflection of both Van de Waals attractions and of increased chain entanglement.

Each shock shows an initially determined strength for the thermoplastic which then increases as slower mechanisms operate within the microstructure. It is believed that the PP and PS show evidence of increased crystallinity at higher pressures and attendant shock temperatures as a result of the formation of iso- and syndiotactic chains triggered by the shock. Further work is under way to identify and isolate these effects.

Acknowledgements We thank Matt Eatwell and Ivan Knapp of Cranfield University for performing the shots in this programme.

References

1. Ashby MF, Jones DRH (1999) Engineering materials 2, 2nd edn. Pergamon, Oxford
2. Mills N (1993) Plastics: microstructure and engineering applications. Butterworth-Heinemann Ltd
3. Carter WJ, Marsh SP (1995) Hugoniot equation of state of polymers. Los Alamos National Laboratory: Los Alamos, New Mexico
4. Millett JCF, Bourne NK (2004) J Phys D: Appl Phys 37:2901
5. Bourne NK (2003) Meas Sci Technol 14:273
6. Rosenberg Z, Yaziv D, Partom Y (1980) J Appl Phys 51:3702
7. Marsh SP (1980) LASL Shock hugoniot data. University of California Press, Los Angeles
8. Millett JCF, Bourne NK, Rosenberg Z (1996) J Phys D Appl Phys 29:2466
9. Rosenberg Z, Bourne NK (2007) Meas Sci Technol 18:1843
10. Bourne NK, Millett JCF, Brown EN, Gray GT III (2007) J Appl Phys (in press)
11. Bat'kov YV, Novikov AD, Fishman ND (1996) In: Schmidt SC, Tao WC (eds) Shock compression of condensed matter 1995. American Institute of Physics: Woodbury, New York, p 577
12. Brown EN, Rae PJ, Trujillo CP, Dattelbaum DM, Gray GT III, Bourne NK (2006) In: Furnish MD et al (eds) Shock compression of condensed matter 2006. American Institute of Physics: Melville, New York, p 196
13. Kargin VA, Tsarevskaya IY, Zubarev VN, Goldanskii VI, Yampolskii PA (1968) Polym Sci USSR 10:3019